HIGH-IMPACT PROPERTY OF POLYKETON/POLYAMIDE-6 ALLOYS INVESTIGATED BY TEM, SAXS, DSC, RAMAN, AND SOLID-STATE NMR

Atsushi Asano[1], *Maiko Nishioka*[2], *Atsushi Kato*[2], *Yohei Takahashi*[2], *Hisahiro Sawabe*[2], *Masazumi Arao*[2], *Shigeo Sato*[2], *Hidenori Sato*[2], *Toshihiro Izumi*[2], *Drozdova Olga*[2], *Daisuke Ishikawa*[2], *Toshinori Hasegawa*[2], *Takeo Okamura*[2], *Kazuya Nagata*[3], *Shigeki Hikasa*[3], *Hitoshi Iwabuki*[3]

1; Department of Applied Chemistry, National Defense Academy, 1-10-20 Hashirimizu, Yokosuka 239-8686, Japan ,
2; NISSAN ARC, LTD., 1 Natsushima, Yokosuka Kanagawa 237-0061, Japan,
3; Industrial Technology Center of Okayama Prefecture, 5301, Haga, Okayama 701-1296, Japan

Introduction

Polymer blends and alloys have already been widely used for engineering purposes. It is well known that the excellent physical properties for a polymer alloy, such as higher impact or modulus, are strongly related to the highly controlled or ordered morphology and homogeneity of utilized materials. Recently, we have found polyketon/polyamide-6 (PK/PA) alloys including over 30 wt% PA show a good impact property rather than the simple addition of the impact energy of both PK and PA.[1] Especially, the PK/PA=60/40 or 70/30 alloys (we refer those alloys as K60A40 and K70A30 hereafter) show a dramatic improvement for the impact property under the conditions of moisture.

In this study, we investigate the relationship between the high-impact property and water adsorption of PK/PA alloys, morphology, and the domain size by solid-state nuclear magnetic resonance spectroscopy (NMR), Raman spectroscopy, differential scanning calorimetry (DSC), transmission electron microscope (TEM), and small-angle X-ray scattering (SAXS).

Experimental

Materials. The polymer alloys are consisted of polyketone (PK, an ethylene/propylene/CO copolymer; Carilon D26HM100, Shell Co.) and polyamide 6 (PA, Amilan CM1017, Toray Ind.). PK/PA alloys were moisture-conditioned by holding them at 50 % or 95 %RH (relative humidity) and a temperature of 296 K for three weeks. Dry test specimens were prepared by drying them in a vacuum at 373 K for 72 h. The moisture absorption rate was measured by using the Karl Fisher method.

Instrumentation. Instrumented Charpy impact tests were conducted according to the procedure specified in JIS K7111 at a temperature of approximately 297 K and at approximately 45% RH. The impact tester used was a CHARPAC-FRII (Yonekura MFG Co., Ltd.) and the obtained data were analyzed by IITMWin19 software (Yonekura MFG Co., Ltd.) designed for processing Charpy impact test data.

High-resolution solid-state ^{13}C NMR spectra were measured using a Varian NMR systems 400WB spectrometer operating at 100.7 MHz for ^{13}C and 400.5 MHz for ^{1}H. The conventional cross polarization (CP) and magic-angle spinning (MAS) with ^{1}H high-power dipolar decoupling technique was used. The radio-frequency field strength for ^{1}H decoupling was 120 kHz and the two-pulse-phase-modulation (TPPM) method was used. The MAS frequency was 16 kHz and the ramped-amplitude CP method was used. ^{13}C chemical shifts were measured relative to tetramethylsilane (TMS) using the benzene carbon signal at 132.07 ppm for solid hexamethylbenzene as an external standard. Solid-state ^{15}N NMR spectra were also measured with MAS = 5 kHz and ^{1}H decoupling frequency of 65 kHz. ^{15}N chemical shifts were measured relative to glycine signal as an external standard.

Raman spectra were measured using a SENTERRATM, Bruker Optics Co. Ltd. spectrometer for the regions of C=O functional group (1709 cm^{-1}) of PK and the NHC=O functional group (1638 cm^{-1}) of PA. An excitation light wavelength was 785 nm.

TEM images were collected using a HITACHI H-800 with an accelerating voltage of 200 kV. The dyeing is done by the phospho tungstic acid solution. SAXS investigations were carried out using a Bruker AXS Nano-STAR diffractometer. Data were collected with Cu Kα radiation (λ = 0.154 nm).

DSC was examined by using a TA Instrument DSC-Q1000 equipment with increasing temperature at rate of 10K·min^{-1} from 273 K to 523 K.

Results and Discussion

Physical property and Morphology. **Figure 1** shows the results of the Charpy impact test and the apparatus. It is noted that the impact total energy of both K70A30 and K60A40 shows noticeable increase under the conditions of moisture, while the value at dry condition does not show such a dramatic improvement. This phenomenon is measured for PK/PA alloys with over 30 wt% of PA. Interestingly, the wet PA does not show such an improvement for impact property. Therefore, this phenomenon should be related to morphology and miscibility between PK and PA. Firstly, we investigate the morphology by TEM image.

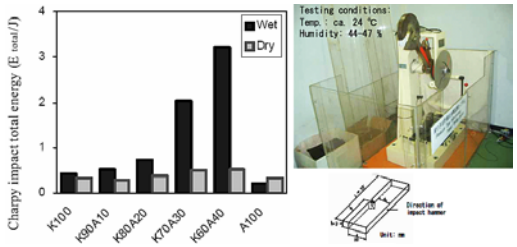

Figure 1. Left: the results of Charpy impact test. Right: Charpy impact test apparatus and dimensions of the utilized sample.

Figure 2 shows both TEM image and SAXS spectra of the K60A40 alloy. The picture of TEM (**Figure 2a**) is magnified by 200,000. This TEM image indicates a lamellar structure and several domains in the alloy. Since the amorphous phase is dominantly dyed, the lamellar structure actually represents the repeat structure of crystalline and amorphous phases. A lamellar thickness seems to be less than 10 to 20 nm. Furthermore, this lamellar exists inside and outside of the domains. For both pure PK and pure PA, and the other alloys including PA less than 30wt%, we did not observe such a lamellar structure from TEM image clearly. These results indicate that the complicate morphology observed for the K60A40 alloy is resulted by a strong interaction between PK and PA. In order to investigate the lamellar thickness, we observed the SAXS spectra of the K60A40 alloy under the conditions of wet and dry.

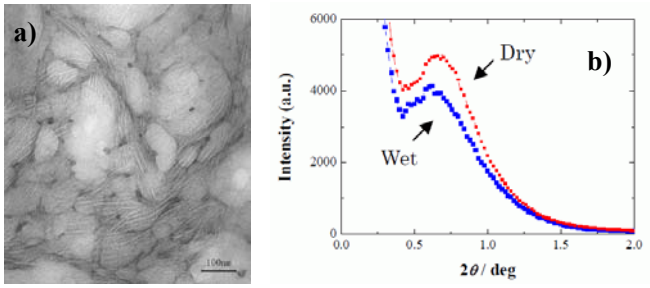

Figure 2. TEM image (a) and SAXS spectra (b) of the K60A40 allloy. A lamellar structure and an island (domain) structure are clearly observed. The black contrast mainly indicates an amorphous phase.

Figure 2b shows the SAXS spectra of dry and wet K60A40 alloys. The peak at 2θ = 0.66° is observed for the dry K60A40 alloy. This indicates that the lamellar thickness can be estimated to be 13.4 nm. On the other hand, the peak for the wet K60A40 alloy shifts slightly toward shorter angle and observed at 2θ = 0.60°. This value represents the lamellar thickness is approximately 14.7 nm. This observation suggests that the lamellar thickness becomes wider in a humid condition. The obtained thickness is in excellent agreement with that observed from TEM image in **Figure 2a**.

It is well known that PA is a semicrystalline polymer and also makes a lamellar structure. However, the SAXS peak which relates the lamellar thickness was observed at 2θ = ca. 1.0°. This means that the thickness is 8.8 nm. Meanwhile, the SAXS signal of PK was not intense at 2θ = ca. 0.7°, although the peak-like plateau was observed. With increase of amount of PA in the PK/PA alloys, the SAXS peak intensity at 2θ = ca. 0.7 become more visible, not at 2θ = ca. 1.0°. Especially, for the K60A40 and K70A30 alloys it appears clearly as a peak. These observations are in good agreement with the

observations of TEM. Furthermore, it indicates that the growth of the lamellar structure of PK is accelerated when PA is included in the alloys over 30 wt%. We also identified the location of PA from nitrogen mapping by an electron energy-loss spectroscopy (EELS).

Miscibility and Interaction. TEM and SAXS observations revealed the morphological image visually. In this section, we discuss the miscibility and interaction from DSC, Raman spectroscopy, and solid-state NMR.

Figure 3 shows the DSC curve of pure PK, the K60A40 alloy, and pure PA: the curves shown here are the second scan. The glass-transition temperature (T_g) of PK is observed at around 283 K and that of PA at around 328 K. For the K60A40 alloy, two distinct T_g peaks are detected, but those T_g's are different from those of homopolymers. One is around 287 K and another around 323 K. This observation shows that the amorphous regions of both PK and PA in the K60A40 alloy are more or less interacted with each other and in close proximity rather than the complete phase separation. Furthermore, the DSC measurements revealed that the melting enthalpy of the alloys decreases much more than those of PK and PA. This indicates that the amorphous region in the alloys increases.

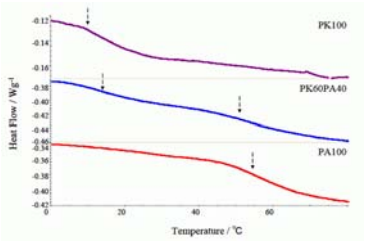

Figure 3. The DSC curves of PK (top), K60A40 (middle), and PA (bottom). The arrows indicate the glass-transition temperature.

Figure 4 shows the Raman spectra of each PK/PA polymer alloy, pure PK and pure PA at the CO region. The peak intensity of the NHC=O functional group (1638 cm^{-1}) increased with amount of PA. Similarly, the peak intensity of the C=O functional group (1709 cm^{-1}) increased with amount of PK. Additionally, the peak of the C=O functional group tended to shift slightly toward the low frequency side with increase of PA. This tendency presumably reflects the interaction between the PK and PA phases.

We focus the full width at half maximum (FWHM) of the Raman shift peak. If there is no interaction between PK and PA, especially between the carbonyl group of PK and the amide group of PA, the FWHM does not show any change. However, **Figure 4** shows that the FWHM values of both CO peaks for PK and PA decrease with increase or decrease of PA. This observation indicates again the existence of the interaction between PK and PA in the alloy.

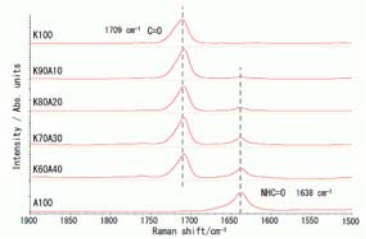

Figure 4. Raman spectra of PK(top), PK/PA alloys, and PA (bottom).

Figure 5 shows the observed high-resolution solid-state CPMAS ^{13}C and ^{15}N NMR spectra of PA and K60A40 samples. The ^{13}C NMR spectra show the relative intensity of amorphous peak decreases under the conditions of moisture. This indicates that the CP efficiency of amorphous phase becomes worse and the water adsorption is predominantly occurred in the amorphous phase. The ^{15}N NMR spectra show that the α-crystalline phase of K60A40 is dominant as compared to that of pure PA; a rapid cooling of PA induced the growth of the γ-crystalline phase in pure PA. This indicates that PK induces the α-crystalline phase of PA in the alloys. The change of crystalline type of PA probably relates the complicate morphology, which is detected by the TEM image, and the high-impact property at wet condition.

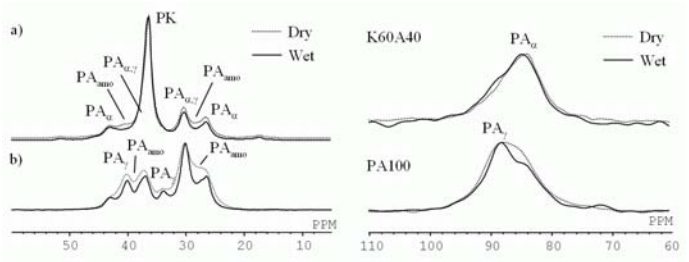

Figure 5. Observed ^{13}C CPMAS NMR spectra (left) and ^{15}N CPMAS NMR spectra (right) of (a) K60A40 and (b) PA for both dry (dotted line) and wet (solid line).

We measured the ^1H spin-lattice relaxation (T_1^H) curves of PK and PA in the dry and wet K60A40 alloys to investigate the averaged domain size from the ^1H spin-diffusion rate, k. **Figure 6** shows the observed T_1^H curves and calculated curves by assuming the two-spin system.[2] The calculated curves are in good agreement with the observed date points. From this simulation, we can deduce the k value to be approximately 1.0 s^{-1}. For the wet alloy, the similar curves were observed and successfully fitted with k = 1.0 s^{-1}. The T_1^H values of the initial decays in the alloy were comparable to those of homopolymers. From the obtained k value, we can estimate the domain size (repeat domain length, L) from the equation of $L = 2\cdot [D/(\pi\cdot k)]^{0.5} / (f_{PK}\cdot f_{PA})$: f is proton mole fraction and D is ^1H spin-diffusion coefficient.[3] The estimated value is approximately 120 nm with D = 700 nm^2s^{-1} for PA.[4] Of course, the value of 120 nm is a rough estimation, because the D value of PK is not considered and it is wonder that domains of PK and PA are constructed repeatedly with each other. However, D value for the common polymers is 100 to 1000 nm^2s^{-1} and DSC and TEM studies show that both polymers are not completely phase separated but they make a domain about several 10 to a few 100 nm. Taking these observations into account, the estimated domain size is reasonable.

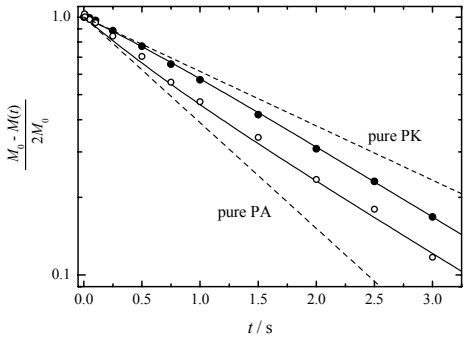

Figure 6. Observed T_1^H curves for pure PK (broken line), pure PA (broken line), and the K60A40 alloy under the dry condition. The solid circles indicate observed T_1^H curve for PK and open circles represent that for PA in the alloy. The solid lines are calculated ones by assuming the two-spin model.

Conclusions

The reasons why the impact property of the wet PK/PA alloys including with over 30 wt% of PA is tremendously high are presumably relating to the elasticity of the amorphous phase of PA under the conditions of moisture, the strong lamellar structure of mainly PK, and the change of crystalline phase for PA from the mixed α and γ phases to α crystalline phase.

References

(1) Kato, A *et al*. submitted to *J. Appl. Polym. Sci*.
(2) Stejskal, E.O.; Schaefer, J.; Sefcik, M.D.; McKay, R.A. *Macromolecules*, **1981**, *14*, 275.
(3) VanderHart, D.L.; McFadden G.B. *Solid State Nuc. Magn. Reson*., **1996**, *7*, 45.
(4) VanderHart D.L.; Asano A.; Gilman J.W. *Chem. Mater*., **2001**, *13*, 3796.